

Temperature and field dependence of the flux-line-lattice symmetry in V_3Si

M. Yethiraj,¹ D. K. Christen,¹ A. A. Gapud,¹ D. McK. Paul,² S. J. Crowe,² C. D. Dewhurst,³ R. Cubitt,³ L. Porcar,⁴ and A. Gurevich⁵

¹Oak Ridge National Laboratory, Oak Ridge, Tennessee 37831, USA

²University of Warwick, Coventry, United Kingdom CV4 7AL

³Institut Laue Langevin, Grenoble, France

⁴NCNR, NIST, Gaithersburg, Maryland 20899, USA

⁵University of Wisconsin, Madison, Wisconsin 53706, USA

(Received 24 May 2005; published 12 August 2005)

In V_3Si , a first-order structural phase transition from hexagonal to square flux-line lattice occurs at approximately 1 T with $H \parallel$ to the a axis. In this paper, we demonstrate the reentrant structural transition in the flux-line lattice, which reverts to hexagonal symmetry as the magnetic field approached $H_{c2}(T)$. This behavior is described very well by a nonlocal London theory with thermal fluctuations. The phase diagram of the flux lattice topology is mapped out for this geometry.

DOI: 10.1103/PhysRevB.72.060504

PACS number(s): 74.70.-b, 74.25.-q, 61.12.Ex

In 1957, Abrikosov predicted the existence of quantized vortices which would form a hexagonal flux-line lattice (FLL) above the lower critical field H_{c1} in type-II superconductors. Small-angle neutron scattering (SANS) and decoration experiments performed on Nb (Ref. 1), tetragonal borocarbides,² and V_3Si (Ref. 3) have shown that the hexagonal FLL actually occurs only at low H close to H_{c1} , while at higher H , the FLL begins to reflect the underlying symmetry of the crystalline lattice (see Fig. 1). This behavior was explained by a nonlocal London theory, which accounts for coupling of vortex supercurrents to the lattice.⁴ Weak nonlocal effects can result in FLL symmetry transitions from square to triangular since the energy difference between the two structures is small ($\approx 2\%$). A similar transition also follows from a modified Ginzburg-Landau (GL) theory with higher-order gradient terms in the vicinity of the critical temperature $T \approx T_c$ (Refs. 5 and 6).

Coupling between the FLL and the crystal results from the basic nonlocal relation⁴ between the current density and the vector potential, $J_\alpha(q) = K_{\alpha\beta}(q)A_\beta(q)$. For \mathbf{H} along the z axis, nonlocality adds a short-range vortex attraction potential $V(x, y)$ with the symmetry of the crystal to the longer-range

isotropic interaction with a spatial extent of order the London penetration depth λ . The kernel $K_{\alpha\beta}$ decays over the nonlocality radius, ρ , which depends on the mean free-path, ℓ , and the BCS coherence length ξ_0 at $T=0$. At low fields, where V is negligible due to the large vortex spacing, the FLL is hexagonal but its orientation is determined by the crystal. With decreasing intervortex spacing, the short-range potential $V(x, y)$ locks the FLL onto certain crystalline directions. This results in orientational FLL transitions due to softening of the rotational elastic modulus of the FLL (Ref. 7), as was indeed observed in borocarbides.⁸

Further, the interaction between nonlocality and vortex fluctuations can result in a new effect manifested by a reentrant square to rhombic transition at high fields. This unusual behavior was explained in the nonlocal London theory as a competition between the square-symmetric nonlocal interaction and the isotropic fluctuations which wash out the nonlocal contribution, thus favoring the triangular FLL to maximize spacing between repulsing vortices.⁹ A similar reentrant transition was also obtained in a GL theory with thermal fluctuations included¹⁰ and the Eilenberger theory taking into account the anisotropy of the Fermi surface.¹¹ The strength

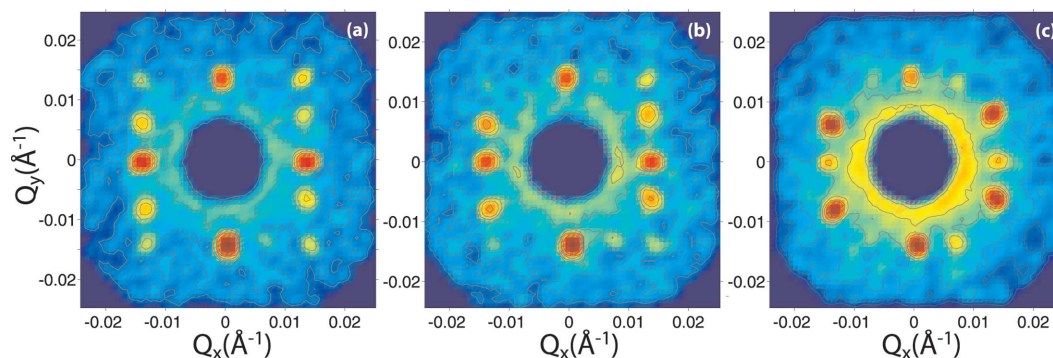


FIG. 1. (Color) The observed diffraction pattern in V_3Si with the field $H=1$ T parallel to the a axis at (a) $T=11$ K, (b) $T=12.5$ K, and (c) $T=14$ K. The fraction of the rhombic FLL at 11 K is less than 10% (the intensity is on a logarithmic scale). The neutron wavelength was 8 \AA , the sample to detector distance = 10 m, and the effective divergence of the beam at the sample was 0.2° . The pattern was obtained by summing over a rocking curve of $\pm 1^\circ$ in 0.1° steps in order to get the different reflections on the Bragg condition.

of the thermal fluctuations and nonlocality is quantified by the parameters,

$$\chi_0 = \frac{16\sqrt{2}\pi^3\lambda_0^2k_B T_c}{\phi_0^2\xi_0}, \quad \zeta_0 = \frac{\pi}{2}\left(\frac{\rho_0}{\xi_0}\right)^2. \quad (1)$$

Here χ_0 is essentially the Ginzburg parameter ($\chi_0 \sim 10^{-3} - 10^{-2}$ for borocarbides and V_3Si), and ρ_0 and λ_0 are the nonlocality radius and the London penetration depth at $T=0$, respectively. The reentrant transition occurs if the mean-squared vortex thermal displacement $\langle u^2 \rangle^{1/2}$ becomes comparable to ξ_0 . This condition can be satisfied even in low- T_c superconductors for which thermal fluctuations are weak $\chi_0 \ll 1$, unlike FLL melting, which requires stronger fluctuations with $\langle u^2 \rangle^{1/2} \approx c_L a(B)$, where $c_L \approx 0.2$ is the Lindemann number. Thus, fluctuations can cause FLL structural transitions even in nearly isotropic superconductors.

In this paper we report SANS measurements of the hex-to-square transition curve $B_{\square}(T)$ in a clean cubic V_3Si single crystal for which nonlocal effects are expected to be most pronounced while the effect of anisotropy of the Fermi surface is very weak.¹ We show directly that the curve $B_{\square}(T)$ is indeed two valued, indicating a reentrant square-to-hex FLL transition at higher fields. The curve $B_{\square}(T)$ is described very well by the nonlocal London theory with thermal fluctuations included.⁹

Our single crystal of V_3Si is a very clean material with a mean-free path of several hundred Å; in addition, it is a rather perfect crystal with a mosaic that is resolution limited in various characterization measurements. The crystal has $T_c = 16.4$ K, $\lambda_0 = 1050$ Å, and $\xi_0 = 35$ Å, as calculated from the observed slope of $B_{c2}(T)$. We carried out SANS measurements of the Bragg scattering from the FLL as a function of temperature and field to explore the FLL symmetry with $\mathbf{H} \parallel$ to the a axis.

The sample was aligned on a diffractometer in the hhl plane (uncertainty $\approx 2^\circ$). Subsequently, the sample was aligned in this plane to have the field parallel to the a axis to within 0.5° on the SANS machine by using the observed metallurgical scattering parallel to the a axis. A horizontal field geometry was used, where the neutron beam is aligned parallel to the applied field and the a axis of the sample. The D11 SANS at the ILL and the NG7 SANS at NIST were used for the measurements. All data points were taken as the sample temperature was changed in a fixed external applied field. The structural differences between heating and cooling to a particular temperature were investigated up to fields of 3 T; no differences were observed. At the lowest temperatures and low field, the FLL had rhombic symmetry, which changed sharply at ≈ 0.9 T to one with square symmetry. A narrow region of coexistence of both rhombic and square contributions was observed and no intermediate structures were seen, suggesting that the transition is first order. The field at which this rhombic-square behavior was observed remained constant for $T \leq 10$ K.

This result is somewhat at variance with STM and μSR work that show a gradual and continuous transition over a much wider field range. We point out that sample quality is extremely important as pinning can smear the transition. Fur-

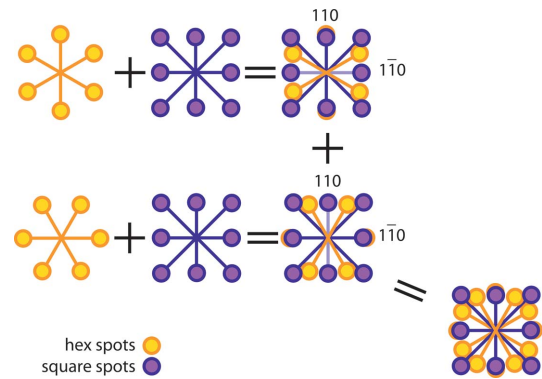


FIG. 2. (Color) A schematic explaining the origin of the multiple peaks visible in a region of phase space that has coexisting square and hexagonal FLL domains. Since the a and b axes are equivalent in this cubic system, two hexagonal domains could be expected to exist. The two square FLL coincide with each other.

ther, a distorted hexagonal lattice persists to higher fields with the field misaligned by a few degrees to the a axis. We presume sample quality and alignment contribute to the observed discrepancy between STM and μSR results and ours.

At fields above which the FLL was square at low temperature, a transition to a slightly distorted hexagonal structure was clearly observed. Again, no intermediate crossover structures between the square and rhombic existed, but there was a regime in which both structures contributed. This transition is markedly different from that reported¹² by Eskildsen *et al.* for the borocarbide system. In their case, although broadening of the azimuthal width of the Bragg peaks was readily apparent, a distinct hexagonal lattice was not the only conclusion, especially in the absence of comparable Bragg-peak intensities at $Q_x=0$ and $Q_y=0$ (for the symmetry equivalent peaks of the two rhombic domains) to the formerly “square” peaks. In the case for V_3Si here, not only did no remnant of the square peaks exist at temperatures near T_c , higher-order peaks of the rhombic lattice were clearly visible (when the sample was at the appropriate angle for the Bragg condition of the higher-order peak to be observed). Azimuthal and radial peak widths in the two phases were not remarkably different, though the FLL rocking curve widths were not resolution limited in either phase. The rocking widths are a measure of the straightness of the flux lines over their length, the azimuthal width measures the perfection of the FLL order, and the radial width measures lattice spacing perfection.

Although, from symmetry considerations, two equivalent domains should exist (as shown in the schematic in Fig. 2), the domain with the plane normal vertical (along one of the symmetry related 110 directions) had considerably higher population than the domain rotated by 90° . It is likely that this is due to the “dominant” 110 being better aligned with the magnetic field, since the sample was rotated about the vertical axis to align the a axis parallel to the applied field using the metallurgical scattering as a guide.

At $T=2$ K, the region of coexistence of square and rhombic lattices was between 0.8 T to just above 1.1 T. At low temperatures and fields, the rhombic (often referred to as “hexagonal”) structure was not always a perfect hexagon;

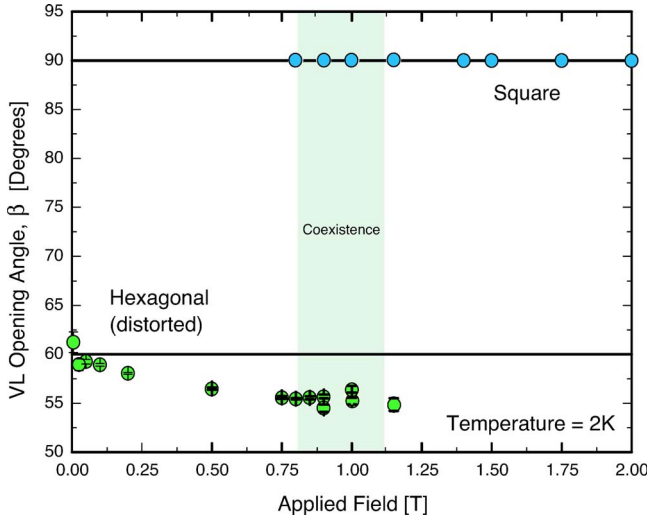


FIG. 3. (Color online) The opening angle (β) as a function of applied field at base temperature=2 K.

small distortions to it were observed. These distortions diminished as the temperature was increased, i.e., the angle between the Bragg spots were closer to (though not exactly) 60° as T_c was approached. The observed opening angle β between the spots above and below the horizontal line at 0.75 T is $55.7 \pm 0.1^\circ$ up to ≈ 8 K. Above this temperature, β changes gradually to 57° at 14 K. Further, β at $T=2$ K was 60° at very low fields (Fig. 3) but monotonically decreased to about 55° just prior to the transformation to square symmetry.

The intensity of the Bragg spots corrected for the Lorentz factor and the form factor is shown in Fig. 4. This intensity should vary as $e^{-Cq^2\xi^2}$. Values for C in the borocarbides were close to 1. Here, in Fig. 4, there appears to be a discontinuity between the intensities of the rhombohedral Bragg peaks and

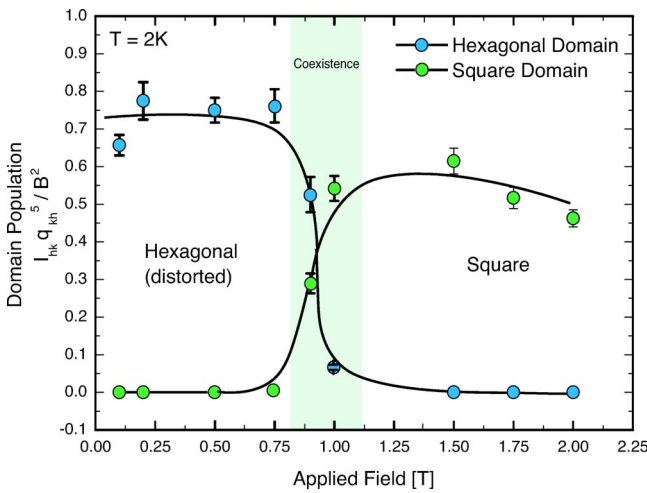


FIG. 4. (Color online) The intensities of rhombic and square FLL intensities as a function of applied field at 2 K are shown. Since the Bragg intensity is proportional $(B/q^2)^2$ from the form factor and further, has a $1/q$ term from the Lorentz factor, Iq^5/B^2 should be constant if all other factors (such as lattice perfection, Debye-Waller factor, for example) remain the same.

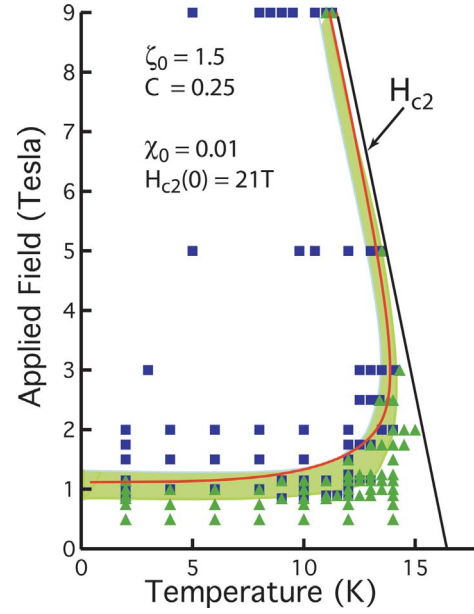


FIG. 5. (Color) The phase diagram of the FLL topology obtained from the diffraction patterns shows that a rhombic FLL (green triangles) dominates at low fields and near $H_{c2}(T)$ curve (black line), while a square FLL (blue squares) is stable at lower temperatures above ≈ 1.1 T. The theoretical transition curve $B_{\square}(T)$ (Ref. 9), is indicated by the solid red line. The shaded region indicates the observed coexistence of both rhombic and square phases.

the square Bragg spots. One explanation is that the FLL is always nucleated as a triangular lattice and then turns into a square FLL at lower temperature. It is possible that the change in symmetry is associated with random disorder, caused by pinning, since at these fields the symmetry change occurs well below T_c . This would give rise to a decrease in intensity from a Debye-Waller-like term, though the disorder is presumably static rather than dynamic. If it is assumed that there is a scale factor difference between the lattices of triangular and square symmetries, the data here are consistent with a much smaller value for the constant $C \approx 0.25$ in the triangular phase and a larger value for $C \approx 0.75$ in the square phase.

At temperatures above 10 K, the rhombic phase persisted to higher fields, giving the appearance of a “nose” on the square-hex transition boundary on the phase diagram. The coexistence region was somewhat broader at the lower fields. At fields of 5 T and higher, a hexagonal component to the FLL was observed only very near T_c . It is seen that the transition field H_{\square} is multivalued at higher temperature. Our data suggest that there may be additional local structures in H_{\square} at around 1 T.

The phase diagram of the FLL topology is summarized in Fig. 5. The line shows $B_{\square}(T)$ calculated from the following equation of the nonlocal London theory with thermal fluctuations:⁹

$$\sum_{mn} \frac{e^{-pg}}{d} \left[(2pmn)^2 + \left(\frac{8m^2n^2}{d} - g \right) \left(p + \frac{1}{d} \right) \right] = 0. \quad (2)$$

Here, $p = [2\pi C + \chi(T) \eta(t, b) / s(b)] b$, $b = B_{\square} / B_{c2}$, $s^2 = b(1 - b)^3 \ln(2 + 1/\sqrt{2b})$, $g = m^2 + n^2$, $d = \mu + g + \zeta(b)(m^2 - n^2)^2$, μ

$=1/2\pi b\kappa^2$, and the parameters $\chi=16\sqrt{2}\pi^3\lambda^2T/\phi_0^2\xi$ and $\zeta=\pi b(\rho/\xi)^2/2$ quantify the amplitude of thermal displacements and the nonlocal corrections. We took $\zeta_0=1.5$, and $\chi_0=.01$ calculated using the observed $\lambda_0=1050$ Å, $\xi_0=35$ Å, and $\kappa=\lambda/\xi=26$. Furthermore, we used the two-fluid temperature dependence for $\lambda(T)=\lambda_0[1-(T/T_c)^4]^{-1/2}$, taking $\rho(T)$ in the clean limit,⁴ and $\xi(T)$ from the observed $B_{c2}(T)$ curve.¹³ The value of $C=0.25$, which accounts for the finite vortex core size in the London theory,¹⁴ was already discussed earlier; it was adjusted to reproduce the observed upper branch of $B_{\square}(T)$ (Ref. 15). In turn, ζ_0 was independently fixed by the position of the lower branch of the $B_{\square}(T)$ curve at low T for which neither thermal fluctuations nor vortex core effects are essential. As follows from Fig. 5, the theory is in excellent agreement with our experimental data.

The contribution of thermal fluctuations is more pronounced in V_3Si than in the borocarbides. Although the parameters χ_0 and ζ_0 are comparable for both materials ($\chi_0=.01$ for V_3Si and 0.007 for $LuNi_2B_2C$), the value of $C\approx 1$ in borocarbides is greater than $C\approx 0.25-0.5$ for V_3Si , as discussed above. This may explain why the gap between the upper branch of $B_{\square}(T)$ and $B_{c2}(T)$ in $LuNi_2B_2C$ (Ref. 12) is

considerably wider than that for V_3Si studied in this work. The larger difference between $B_{\square}(T)$ and $B_{c2}(T)$ in borocarbides can also result from the essential anisotropy of the Fermi surface,¹¹ which is absent in V_3Si (Ref. 1).

In conclusion, we present SANS measurements of the hexagonal-to-square structural transitions in the vortex lattice in V_3Si . We report a clear indication of the reentrant square-to-rhombic transition vortex lattice transition at higher fields approaching $B_{c2}(T)$. Our results are described well by a nonlocal London theory with thermal fluctuations included.

Many thanks to V. G. Kogan for useful discussions and to David Bowyer at the ILL, and D. C. Dender, E. M. Fitzgerald, and B. S. Greenwald at NIST. This work was supported at Oak Ridge National Laboratory, which is managed by UT-Battelle LLC, under Contract No. DE-AC00OR22725 for the U. S. Department of Energy. The Warwick Group wish to acknowledge the financial support of the EPSRC, UK. Work at UW was supported by NSF under MRSEC Grant No. DMR-0079983.

- ¹*Anisotropy Effects in Superconductors*, edited by H. Weber (Plenum, New York, 1977); D. K. Christen *et al.*, Phys. Rev. B **21**, 102 (1980).
- ²U. Yaron *et al.*, Nature (London) **382**, 236 (1996); M. R. Eskildsen *et al.*, Phys. Rev. Lett. **78**, 1968 (1997); D. McK. Paul *et al.*, *ibid.* **80**, 1517 (1998); H. Sakata *et al.*, *ibid.* **84**, 1583 (2000). L. Ya. Vinnikov *et al.*, Phys. Rev. B **64**, 024504(R) (2001).
- ³M. Yethiraj *et al.*, Phys. Rev. Lett. **78**, 4849 (1997); **82**, 5112 (1999); C. E. Sosolik *et al.*, Phys. Rev. B **68**, 140503(R) (2003); J. E. Sonier *et al.*, Phys. Rev. Lett. **93**, 017002 (2004).
- ⁴V. G. Kogan *et al.*, Phys. Rev. B **54**, 12386 (1996); V. G. Kogan *et al.*, Phys. Rev. Lett. **79**, 741 (1997); also in *The Superconducting State in Magnetic Fields*, edited by C. A. R. Sa de Melo, Series on Directions in Condensed Matter Physics, Vol. 13 (World Scientific, Singapore, 1998).
- ⁵Y. De Wilde *et al.*, Phys. Rev. Lett. **78**, 4273 (1997).
- ⁶I. Affleck, M. Franz, and M. H. S. Amin, Phys. Rev. B **55**, R704 (1997).

- ⁷P. Miranovic and V. G. Kogan, Phys. Rev. Lett. **87**, 137002 (2001).
- ⁸S. J. Levett, C. D. Dewhurst, and D. McK. Paul, Phys. Rev. B **66**, 014515 (2002); M. R. Eskildsen *et al.*, Phys. Rev. Lett. **86**, 320 (2001).
- ⁹A. Gurevich and V. G. Kogan, Phys. Rev. Lett. **87**, 177009 (2001).
- ¹⁰A. D. Klironomos and A. T. Dorsey, Phys. Rev. Lett. **91**, 097002 (2003).
- ¹¹N. Nakai, P. Miranovic, M. Ichioka, and K. Machida, Phys. Rev. Lett. **89**, 237004 (2002).
- ¹²M. R. Eskildsen *et al.*, Phys. Rev. Lett. **86**, 5148 (2001).
- ¹³J. R. Thompson (private communication).
- ¹⁴A. Yaouanc, P. D. de Reotier, and E. H. Brandt, Phys. Rev. B **55**, 11107 (1997).
- ¹⁵Here we define C as conventionally used for the analysis of SANS data. This value of C should be multiplied by 2 to match the definition of C in Ref. 9.